Allianz Fahrweg Normalspur / Genfergasse 11, CH-3001 Bern / info@allianz-fahrweg.ch / allianz-fahrweg.ch

Variability of Track Decay Rate Measurements

Variation of TDR measurements according to EN 15461 on prestressed monobloc concrete sleepers with continuously welded rails 60E1 or 60E2

June 2025

Impressum

Author
Urs Schönholzer, https://orcid.org/0000-0001-4333-169X

Publisher
Allianz Fahrweg Normalspur, Bern, Switzerland, https://allianz-fahrweg.ch

ISBN
978-3-907456-01-9

URL

https://www.allianz-fahrweg.ch/publications/9783907456019.pdf

Citation
Urs Schönholzer, «Variability of Track Decay Rate Measurements», Allianz Fahrweg Normalspur, Bern, 2025, ISBN 978-3-907456-01-9, https://www.allianz-fahrweg.ch/publications/9783907456019.pdf

Version
1.1.0

Internal Reference
PRJ-100-043-202

ALLIANZ FAHRWEG

Content

Abstract

Measuring the track decay rate (TDR) according to EN 15461 is an established practice for assessing the acoustic properties of railway tracks. This measurement is a prerequisite for track sections that are used to assess the pass-by noise of rail vehicles according to EN ISO 3095. Also, in normal operation of railway lines TDR measurements are regularly performed, often in combination with pass-by measurements to assess the noise aspects of railway renewal or expansion projects or to test the effectiveness of noise mitigation measures on the superstructure. Whereas it is common practice to measure several pass-by noise events to account for the variability of individual trains, TDR measurements are usually just made once per site. This single measurement is then considered to be representative for that site, or sometimes even across individual sites with the same general type of sleepers and rail profiles. There is not much data available about the variation of various individual TDR measurements. This report uses two datasets of repeated TDR measurements by two different suppliers at a total of eight different locations in the Swiss railway network with very similar conditions in terms of track geometry and superstructure. More than 200 third-octave spectra for the vertical and horizontal TDR are present in the data. The variation of the obtained results on nominally identical superstructure is analysed and discussed.

1 Introduction

Track Decay Rate measurements according to EN 15461 are used to characterize the dynamic properties of a section of rail. For the measurement, the rail is excited by hitting it with an impact hammer and it is analysed how the response at a sensor mounted on the rail changes with increasing distance between the impact and the sensor. A track section with high TDR can dissipate the energy of the impact on a rather short distance of rail through the rail fastening system into the sleeper and the rest of the track structure. A rail with a low TDR is not able to dissipate the energy easily and radiates more energy in the form of airborne noise (Thompson, 2009). The rail pads, mounted between the rails and the concrete sleepers, have a significant influence on the TDR. A soft rail pad with a lower static stiffness isolates the rail from the sleeper to a higher extent and results in a lower TDR than a stiff rail pad (Thompson, 2009).

The TDR is mainly a property of the superstructure design that does not change too much over the lifespan of a track. As it is predominantly influenced by the rail pad and the rest of the fastening system, it is stable over time if the relevant components do not change their properties, e.g. due to ageing (Venghaus, 2018). This contrasts with acoustic rail roughness, another parameter defined with a limit curve in EN ISO 3095, that is considered to change more substantially due to developing corrugation over the lifespan of a rail between grinding cycles (Grassie, 2009).

There are several factors that influence a TDR measurement in practice. To perform the measurement, it is possible to keep the location of the impact constant and move the accelerometer farther away with each step (SN EN 15461, 2011). A second possibility is to keep the sensor fixed and to change the position of the impact. The second fundamental choice is the method of fixation of the sensor to the rail. One option is to use glue for this purpose. This takes some time for the glue to harden and to remove the sensor after the measurement is completed. A very easy method of attaching the sensor to the rail is by using a magnetic base plate. But there are some reasonable doubts concerning this method, without prior verification that the sensor attached by the magnet and base plate will show equally well coupling to the rail compared to the fixation by gluing. When the sensor is fixed by glueing it to the rail, the method with moving the impact position needs to be chosen, as glueing the sensor several times per measurement is not practically feasible.

Rail temperature is another influence on the TDR measurement. As nowadays virtually all tracks use continuously welded rail (CWR), the tension within the rail varies with temperature. The target temperature for a non-tensioned rail in Switzerland is 25°C. Below this temperature, tensile forces occur in the rails, above this temperature, compression forces are present in the CWR. Therefore, the temperature of the rail, which might differ considerably from the ambient temperature, is usually recorded during TDR measurements.

TDR is also an input parameter in various models for railway noise prediction (Venkataraman, Rumpler, Leth, Toward, & Bustad, 2022). An intrinsic issue with TDR measurements is that the measurement is performed without a train on the track. But the rolling stock influences the coupling of the rail to the sleepers with its weight. The measurement of an unloaded track can underestimate the TDR of the rail underneath a rolling train.

Generally, TDR measurements are expensive, as they need an intervention in track and require the track to be closed for operation during the data acquisition. The actual measurement in track with the sensor and the impact hammer might be done in about one hour. But with installation of the data acquisition electronics and the required cabling, a measurement usually takes half a day on site, in total roughly a day including travel time. Compared with noise measurements this is rather expensive for one set of data. Therefore, it is understandable that repeatability and variability data for TDR measurements is not abundantly available.

The aim of this study is to take the already available measurement data collected over a period of 12 years on the Swiss railway network and to analyse its variability. When reporting the superstructure on which the measurement has been performed, often there is only the sleeper type, and the rail profile specified. It is already clear from theory, that the rail pads also have a major influence. In the data analysed in the present study, rail pads have been always the same. But there might be other factors that need to be considered or reported.

All data used in the present study comes from measurements on tracks with prestressed monobloc concrete sleepers (SN EN 13230-2, 2016) and CWR with vingole rails of a linear weight of 60 kg/m, as-rolled profiles 60E1 and 60E2 (SN EN 13674-1, 2017).

2 Field measurements

The present study is based on measurement data that was acquired on the network of Swiss Federal Railways in the years 2012 to 2023. The data was collected at eight locations on the main east-west and north-south railway corridors in Switzerland. In six of these locations, permanent railway noise monitoring stations are operated by the Swiss Federal Office of Transportation. Primary purpose of these sites is the constant surveillance of noise emissions. For quality control, TDR and acoustic rail roughness are measured once per year at all sites. Figure 1 shows one such site located between Zürich and Winterthur with the noise monitoring system. The two microphones can be seen on both sides of the tracks. Data acquisition is carried out in the grey box in the background.

Figure 1: Photo of a noise monitoring station on the line between the cities of Zürich and Winterthur in Switzerland. Photo credit: own work by the author.

2.1 Track Characteristics

All sites are normal-gauge double-track lines with the following characteristics.

- Tangent track without a substantial gradient.
- 60E1/E2 rails with 60 kg/m and R260 steel grade.
- Prestressed concrete monobloc sleepers without any under-sleeper pads – B70 installed between 1970 and 1990 and B91 as of 1991 – sleeper spacing is 0.60 m.
- Ethylene-vinyl acetate (EVA) rail pads with a static stiffness of approx. 700 N/mm, known as “stiff” rail pads, and a thickness of 7 mm.
- Epsilon-type rail clamps of two types irrespective of the sleeper type.

2.2 Dataset for Supplier 1

The TDR measurements were performed once a year by the supplier in question, always between September and November, at six locations from 2016 to 2023 and in accordance with EN 15461. The chosen measurement method consists in repeatedly hitting the rail with an automated mechanical impact system at a fixed location and measuring the response with mobile sensors. Two sensors are moved along the rail to simultaneously measure the signal in both directions of the impact. A third sensor is placed next to the impact hammer to verify the uniformity of the impulse strength introduced into the rail. The rail temperature was recorded but had little influence on the results.

The initial dataset consists of 184 third-octave spectra of vertical and horizontal TDR and are classified by date and by individual rail. The distinction was made between the two different types of sleepers and the two fastening systems. Some tracks were renewed after 2016 and the information on the previous sleepers was unavailable and, hence, the associated measurements were excluded from the data set.

2.3 Dataset for Supplier 2

The third-octave spectra have been recorded at a total of six locations and include about 40 third-octave spectra of vertical and horizontal TDR, respectively. Four of these locations with a total of 20 spectra in each direction coincide with four of the locations also measured by Supplier 1. This dataset was acquired between June and July 2012. One of the remaining two locations has four spectra and was also measured in the summer of 2012. The bulk of the data for Supplier 2 was measured at one single site with 15 measurements. That site was used for a field study on rail dampers and TDR was measured multiple times in several sections of about 1 km of tangent track in the years from 2012 to 2015. Only measurements without rail dampers installed were considered for the present study.

Supplier 2 uses a manual hammer for the excitation of the rail and leaves the sensor installed at the identical location during the measurement. The hammer is equipped with a sensor to measure the impact force when exciting the rail. The signals of the hammer and at the stationary sensor are monitored during data acquisition and irregular signals are discarded and the measurement at the respective position are repeated. Compliance with SN EN 15461 has been confirmed.

2.4 General comments

Data preparation and analysis was performed with the software packages R (R Core Team, 2024) and ggplot2 (Wickham, 2016).

As aforementioned, the rails and rail pads are identical for all measurements. The limit curves of vertical and horizontal TDR according to EN ISO 3095 are shown in the plots to guide the eye. The measurements are performed on rails in normal operation, therefore the limit curve for track used for the homologation of vehicles does not apply.

2.5 Idealisation and limitations

The tracks were in service for the entire duration of the study. There were some maintenance activities, such as rail reprofiling or ballast tamping. These events were not recorded and their influence on the TDR spectra was not investigated.

The rails at the measurement sites were installed as a mix of rolling profiles 60E1 and 60E2, based on the time of installation. The difference between the two profiles is minimal. Moreover, the railheads are subject to wear-and-tear from traffic and rail grinding changing the cross-sectional area of the rail, albeit limited for this time span. For the ease of read, the rail profile is referred to as 60E2 hereinafter.

3 Results

3.1 Dataset for Supplier 1

Figure 2 shows the TDR measurements with a colour code for the two types of sleepers. The red curves are from the newer and current B91 sleeper type. The blue curves come from the older B70 sleeper variant installed before that. It is important to note that this age can only be attributed to the sleeper itself. Rails and rail pads will very likely have been changed once or even multiple times since the B70 sleepers have been placed in track. It can therefore not be directly concluded that ageing or degradation of the rail pads is a probable root cause for the effects seen below.

The vertical TDR in Figure 2a shows virtually no similarities between all the recorded curves if the colour of the two subsets is ignored and the dataset is viewed in its entirety. There are responses in the range of 1 to 30 dB/m present over the whole frequency range. It looks like any TDR curve is possible from the rails under test. The dataset has so much variability, that averaging over all the spectra would give arbitrary results. If the distinction into both subsets is made, the vertical TDR shows no apparent difference of the curves up to the 630 Hz frequency band (upper end of the central horizontal plateau of the black ISO 3095 limit curve). In that lower part, all the curves show substantial variation. In the range between 630 and 2,000 Hz, a distinct separation of the two sets is visible, with the older (blue) variant of the sleepers showing a consistently lower TDR. This separation disappears again above 2,000 Hz.

Figure 2b shows the horizontal TDR data. There is a much more concise pattern for the measurements, already without the split into the two subsets. A common general trend in the frequency response is visible for the entire dataset. Only at the edges of the relevant frequency range, below 300 Hz and above 3,000 Hz, the curves start to diverge. But this happens to a smaller extent than for the vertical TDR measurement. Looking at the differences of the two subsets shows a separation only up to the 400 Hz band, with the older sleeper type showing lower decay rates. For the higher frequency bands, there are differences visible, for example in the 3,000 Hz band. Just from the general visual impression of Figure 2b it seems that averaging the two individual subsets and discussing these two curves could give a meaningful result if the subsets would be compared to each other.

As stated above, it is not the purpose of the analysis to assess compliance of the tracks with the limit curve in EN ISO 3095. It is still noted, however, that except for a few potential outliers at individual frequencies, all the red curves for the horizontal TDR in Figure 2b stay well above of the black limit curve.

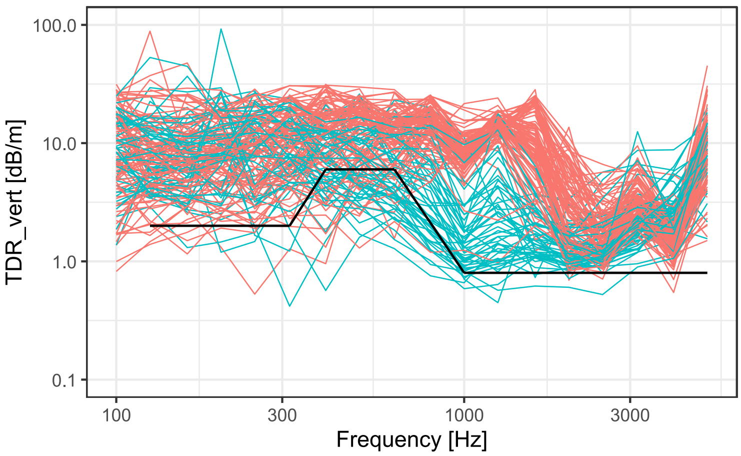

(a)

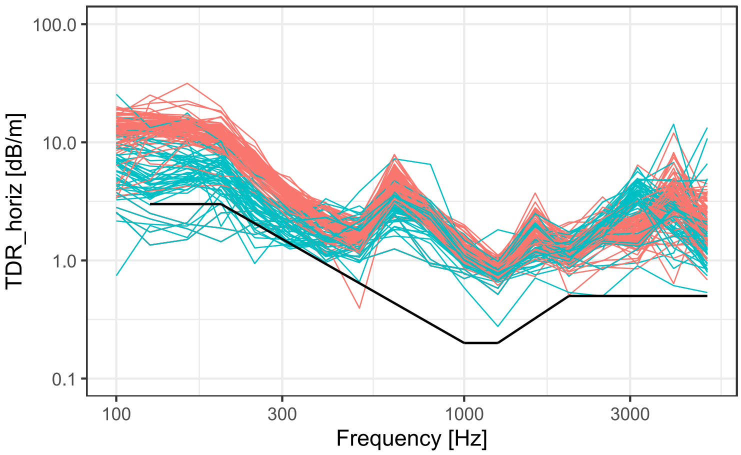

(b)

Figure 2: TDR distinguished by the two types of monobloc concrete sleepers in the sample, the red curves are from the newer sleepers younger than 1991, the blue lines are from the older sleepers, N_{red} = 94, N_{blue} = 50: (a) vertical and (b) horizontal.

Figure 3 shows the red subset from Figure 2 in the form of boxplots. In this view, the coherence of individual third-octave spectra is lost, and the variation of the data is analysed independently for each of the 18 frequency bands.

The boxplots of the vertical TDR data in Figure 3a show the large spread of the individual values that was already visually apparent in Figure 2a. At 800 Hz and below, the boxes are tall and show considerable overlap in horizontal direction. It is probable that a suitable statistical test would lead to the result that there is no significant difference between the individual frequency bands. Just the 1,250 Hz band shows a relatively narrow distribution of values. Above that frequency, the boxes grow rather tall again.

Figure 3b with the horizontal TDR shows quite a strong contrast in the size of the individual boxes compared to the vertical TDR data. There is no substantial difference in the spread of the measurement data for all the individual frequency bands present. It is surprising to see such a variation in the distribution of results, given that both the vertical and the horizontal TDR data for each rail have been collected by the same people, at the same time of year, with the same equipment. Numerical values for the boxplots can be found in the appendix.

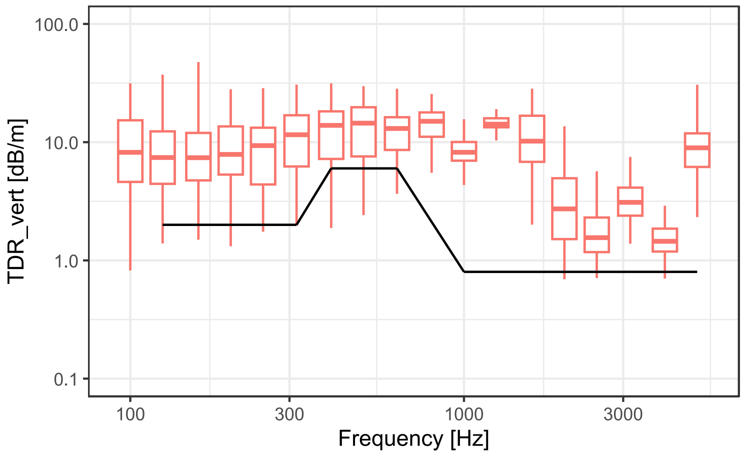

(a)

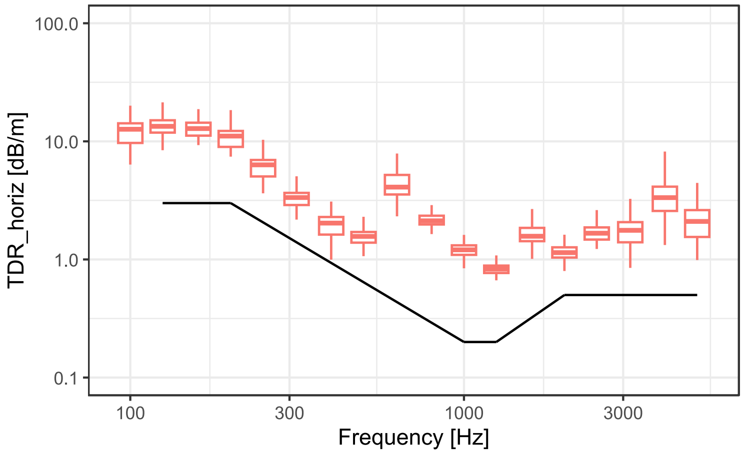

(b)

Figure 3: TDR data of the newer and current version of concrete sleeper (red subset in Figure 2) displayed as boxplots. Outlier points are omitted in the graph for clarity. Scale of the vertical axis identical to Figure 2, N = 94: (a) vertical and (b) horizontal

The possibility of TDR variation with time is assessed in Figure 4. The four individual graphs show all four rails of the two tracks at one of the measurement locations. Identical colours of the spectra denote one year of measurement. There is no trend visible for the four rails at the location to show an identical variation over time in the lower frequency bands that might offer a time-based explanation for the large spread of measurement values. If degradation of track components was the root cause of the variation, a similar sequence of colours should be visible in the graphs, which is not the case. In addition, the span of eight years is considered a relatively small amount of time, as the life of the components regularly is three times this duration.

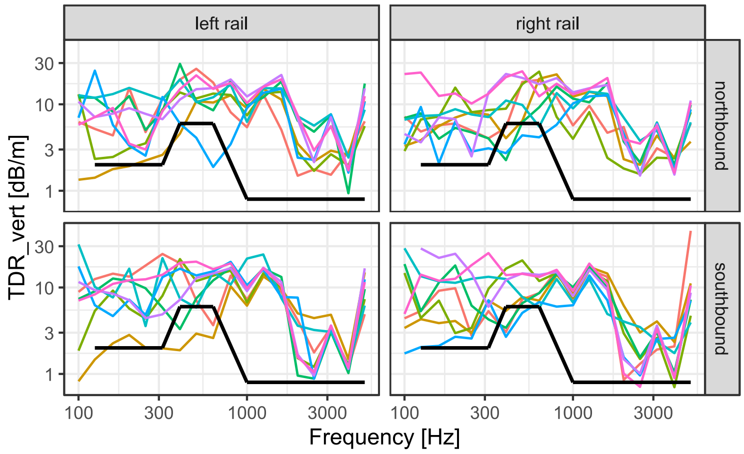

Figure 4: All four individual rails of one location over the span of eight years, vertical TDR. Similar colour indicates identical year of measurement. N = 8.

3.2 Dataset for Supplier 2

The second dataset contains third-octave spectra for a variety of sleeper types and suppliers. For this analysis, the focus was placed on a variability comparison of measurements on a superstructure identical to the data in the red curves from Figure 2 measured by a second supplier.

It can be seen in Figure 5a that the variation of vertical TDR in the range from 300 to 1,000 Hz is substantially narrower compared to what is shown in Figure 2. Even though there are less spectra present in the data the difference seems evident. At frequencies below 300 Hz the variation of the individual spectra becomes larger also in this dataset. The variations for Supplier 2 seem to be a bit larger for frequencies above 1,250 Hz.

The variation in the recorded spectra from Supplier 2 for the horizontal TDR in Figure 5b is also narrower than for the measurements in vertical direction. But the difference is considerably smaller than that for Supplier 1. The boxplots in Figure 6 confirm the narrower distribution of the recorded spectra. The numerical values of the boxplot bounds can be found in the appendix.

The data for Supplier 2 also confirms the statement made above that the superstructure under test in the experiments hardly ever crosses the limit curve of EN ISO 3095.

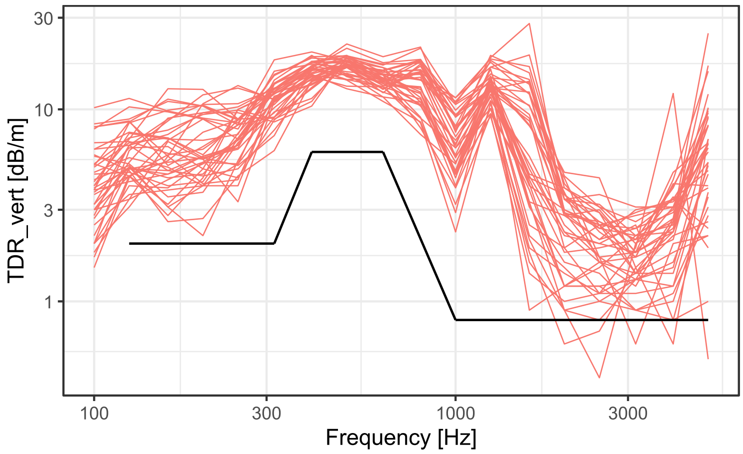

(a)

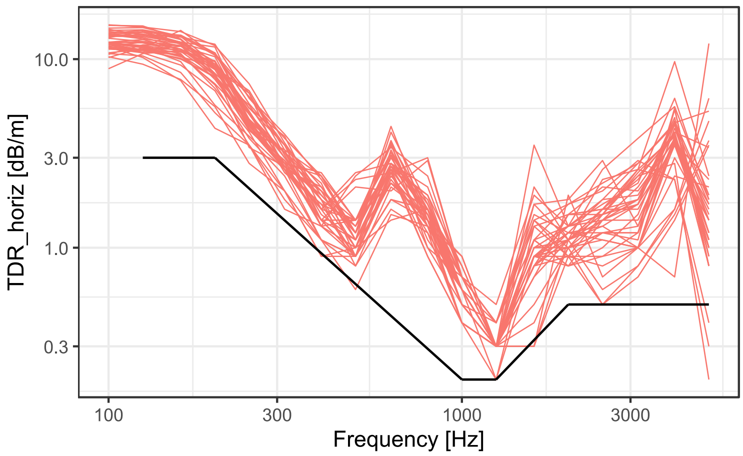

(b)

Figure 5: TDR spectra for Supplier 2. Superstructure of tracks is identical to the red curves in all previous figures. N = 39; (a) vertical and (b) horizontal

4 Discussion

4.1 Variability for sleeper types

Figure 2 shows a significant difference in vertical and horizontal TDR for two types of prestressed monobloc concrete sleepers. The rail profile and rail pads are identical for both types. This systematic difference has been observed in the past, but its root cause has not been comprehensively evaluated. Main reason for the lack of further investigation was that the older sleepers have last been produced around 1990 and track that has been equipped with older production lots form the 1970s is regularly renewed with the current sleeper type. Therefore, infrastructure managers as well as the authorities did not have a profound interest in finding the root cause of the effect. As the newer sleepers show a higher TDR in both vertical and horizontal direction, the origin of the difference was not investigated further.

4.2 Variability of vertical TDR from Supplier 1

The substantially larger variation of vertical TDR compared to the horizontal values as shown in Figures 2 and 3 has not been found in recent discussions in the field. Of course, one possibility to mitigate the fluctuating vertical values would be calculating the energetic average of the vertical TDR for two rails of a track, or even for the entire dataset. This would visibly eliminate some variation and might be considered the true, or at least more reliable value of the vertical TDR. However, if there is a large statistical component in the results, the resulting average or mean value would not have a significant meaning.

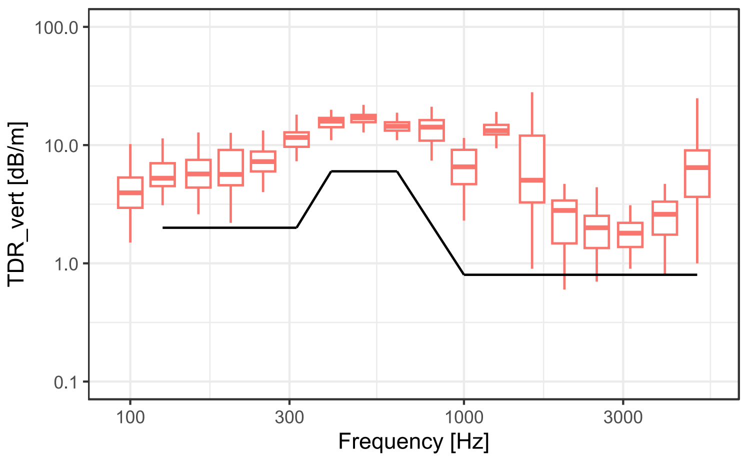

(a)

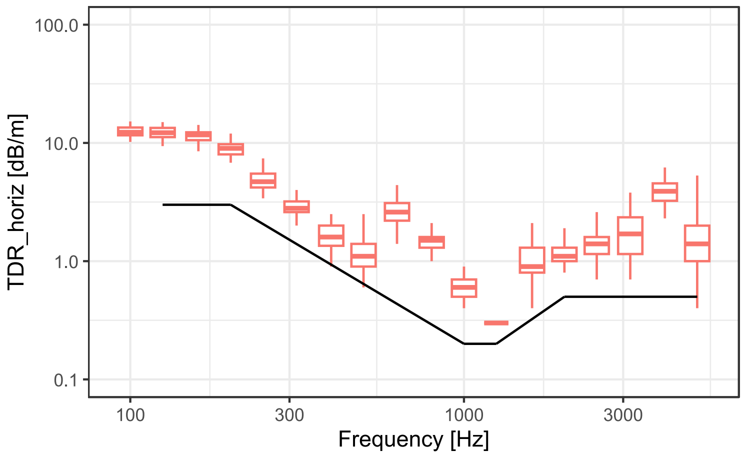

(b)

Figure 6: Boxplot of the data shown in Figure . Numerical values see appendix. N= 39; (a) vertical and (b) horizontal

As the boxplots for the 1,000 Hz and 1,250 Hz bands in Figure 2a are about the same size as all the boxplots for the horizontal TDR of Figure 2b, it seems to be possible to achieve a similarly narrow distribution of the measured values, just not for the entire frequency range. Both, vertical and horizontal TDR were measured with the same sensors and the same automated impact hammer was used. This also means, that the excitation introduced into the rail has been the same for both directions of TDR measurement.

The standard EN 13674-1 defines the dimensions and tolerances for vignole rails. Some other characteristics of the various geometrical cross sections are also listed, for instance the moment of inertia. For the 60E2 rail profile the moment of inertia for a load in vertical direction is given as 3,021.5 cm^4 and for a horizontal load as 510.5 cm^4. There is a factor of six of difference in the resistance of the rail for bending in vertical or horizontal direction, respectively. If this also affects the transmission of the impulse used for determining the TDR, there is more resistance in vertical direction, and an identical impulse will generate less amplitude in the signal along the rail than in horizontal direction. This would lead to a significantly lower signal to noise ratio for the vertical TDR and can be an explanation for the observed effect. If there is a vertical resonance in the rail in the

1,000 – 1,250 Hz range, the signal would be strong in that range also for the vertical TDR. This would lead to a much better signal to noise ratio and could be the reason for the rather narrow spread of values in that range. As the reported dB/m are relative units, there is no conclusion possible about the actual amplitudes that have been recorded by the sensor in both directions.

The raw data for the measurements was not available for the present study. Therefore, testing this hypothesis was not done and will be undertaken in further work.

Data collected by Supplier 2 in Figures 5 and 6 show that at least for the range of 300 to 1,000 Hz a significantly better correlation of individual measurements in vertical direction can be achieved at various locations with the same superstructure. Horizontal TDR is reported much more consistently by both suppliers.

In the range above 1,250 Hz there seems to be the possibility for a systematic difference in average values between measuring methods. The cause for this cannot be assessed with the available data.

It would be beneficial to run a round-robin measurement campaign with different contractors to see if the effect of large variation in vertical TDR persists over different teams conducting the measurement according to EN 15461. This has already been done for measurements of acoustic rail roughness according to EN 15610, where results for repeatability and reproducibility are published in TR 15874.

4.3 Use of TDR in Models

It has always been known that just using the rail profile and sleeper type to characterize a superstructure for assessing its TDR is not sufficient. The properties of the rail pads play an important role and the respective data must be mentioned as well when reporting on measurements. The present study shows, that also identical rails and rail pads can have a different vertical and horizontal TDR response on two types of prestressed concrete monobloc sleepers. This plays a role when employing models that use a TDR curve as input to determine network-wide noise emissions of railways, as for instance mandated by the EU noise directive. If a model uses TDR, all relevant superstructure inventory data needs to be present to calculate the correct emissions and immissions for a railway line. Of course, the error made by for instance using one TDR curve for all concrete sleepers must be put in relation with all other uncertainties of the modelling chain. It does not make sense to meticulously record each type of sleeper in a network when other uncertainties in the modelling chain play a much bigger role.

5 Conclusions

Third-octave spectra measured on comparable superstructure by two different suppliers have found to show a considerable difference in variability amongst individual measurements on tracks with similar components. For a client contracting TDR measurements, it is not possible to assess the quality of different suppliers before or after the measurements. It is unusual to have such a large number of different measurements as a base for an analysis as it was performed here. Before aggregating all the individual measurements over the years, it has not been obvious that the spectra show such a variation. None of the present data has been collected for acceptance tests of rolling stock, but a variation of this magnitude in the data could have an influence if this is also the case with other suppliers. It should mainly be the duty of these suppliers to compare their measurement data over time and use it for quality assurance and plausibility before submitting results to their clients.

The root cause for the observed behaviour could not be found by analysing the third-octave spectra. This will require further work with raw data and further findings maybe even need to be considered in an upcoming revision of the corresponding standard.

References

Grassie, S. L. (2009). Rail corrugation: Characteristics, causes, and treatments. *Proceedings of the Institution of Mechanical Engineers, Part F: Journal of Rail and Rapid Transit, 223*(6), 581-596. doi:10.1243/09544097JRRT264

R Core Team. (2024). R: A Language and Environment for Statistical Computing. Vienna, Austria: R Foundation for Statistical Computing. Von https://www.R-project.org/ abgerufen

SN EN 13230-2. (2016). *Railway applications - Track - Concrete sleepers and bearers - Part 2: Prestressed monoblock sleepers*. Brussels, Belgium: CEN.

SN EN 13674-1. (2017). *Railway applications - Track - Rail - Part 1: Vignole railway rails 46 kg/m and above*. Brussels, Belgium: CEN.

SN EN 15461. (2011). *Railway applications - Noise emission - Characterisation of the dynamic properties of track sections for pass by noise measurements*. Brussels, Belgium: CEN.

SN EN ISO 3095. (2013). *Acoustics - Railway applications - Measurement of noise emitted by railbound vehicles*. Brussels, Belgium: CEN.

Thompson, D. J. (2009). *Railway noise and vibration: mechanisms, modelling and means of control.* Amsterdam Boston: Elsevier.

Venghaus, H. (2018). Ageing Cuts Down the Track Homogeneity Causing Differences Between Calculations and Measurements of Railway Noise. *Noise and Vibration Mitigation for Rail Transportation Systems* (S. 239-249). Cham: Springer International Publishing. doi:10.1007/978-3-319-73411-8_17

Venkataraman, S., Rumpler, R., Leth, S., Toward, M., & Bustad, T. (2022). Improving strategic noise mapping of railway noise in Europe: Refining CNOSSOS-EU calculations using TWINS. *Science of The Total Environment, 839*, 156216. doi:10.1016/j.scitotenv.2022.156216

Wickham, H. (2016). *ggplot2: Elegant Graphics for Data Analysis.* New York: Springer-Verlag. Retrieved from https://ggplot2.tidyverse.org

Conflict of Interest

The authors declare that they have no competing financial interests or personal relationships that could have influenced the work reported in this document.

Acknowledgement

Swiss Federal Office for Transportation for providing part of the analysed data.

Appendix: Boxplot numerical data

Outliers are not displayed in the plots but are present here.

Table 1: Supplier 1 TDR vertical, data for Figure 3a.

Freq-band	0%	25%	50%	75%	100%
100	0.822	4.61	8.2	15.3	31.5
125	1.39	4.44	7.42	12.3	88.4
160	1.16	4.75	7.39	12	47.6
200	1.32	5.32	7.88	13.6	28
250	0.528	4.39	9.36	13.3	28.6
315	1.27	6.23	11.6	16.9	30.7
400	0.956	7.21	13.9	18.2	31.4
500	1.3	7.58	14.5	19.7	29.8
630	1.56	8.6	13.1	16.3	28.3
800	1.19	11.1	15	17.8	25.5
1000	1.24	6.97	8.21	10	21.6
1250	0.975	13.4	14.2	15.9	24.1
1600	1.23	6.82	10.2	16.8	28.4
2000	0.693	1.51	2.73	4.96	13.6
2500	0.709	1.18	1.56	2.31	6.62
3150	1.38	2.39	3.1	4.13	9.49
4000	0.546	1.19	1.45	1.86	5.38
5000	1.5	6.17	8.96	11.9	45.2

Table 2: Supplier 1 TDR horizontal, data for Figure 3b.

freq-band	0%	25%	50%	75%	100%
100	2.51	9.69	12.7	14.2	20
125	1.35	11.9	13.4	15.1	25.1
160	1.5	11.2	12.8	14.4	31.6
200	1.44	8.98	11.1	12.3	19.9
250	1.66	5.04	6.32	6.96	10.3
315	1.88	2.89	3.34	3.66	5.06
400	0.997	1.62	2.03	2.29	3.09
500	0.394	1.39	1.57	1.71	2.3
630	1.25	3.55	4.1	5.2	7.89
800	0.901	1.98	2.12	2.35	3.16
1000	0.701	1.09	1.21	1.32	2
1250	0.516	0.768	0.829	0.887	1.11
1600	0.73	1.43	1.57	1.85	3.72
2000	0.507	1.04	1.14	1.27	2.11
2500	0.836	1.47	1.67	1.87	3.45
3150	0.849	1.4	1.76	2.07	6.42
4000	0.637	2.57	3.34	4.13	12
5000	0.685	1.55	2.1	2.62	4.45

Table 3: Supplier 2 TDR vertical, data for Figure 6a.

freq-band	0%	25%	50%	75%	100%
100	1.5	2.95	3.95	5.32	10.2
125	3.1	4.5	5.25	7.02	11.4
160	2.6	4.38	5.7	7.5	12.8
200	2.2	4.57	5.65	9.1	12.7
250	3.3	6	7.25	8.83	13.3
315	6.1	9.67	11.6	12.8	18.1
400	10.4	14.2	16	17	19.9
500	12.8	15.6	17	18	21.9
630	11	13.3	14.4	15.6	18.8
800	7.4	10.9	14.2	16.3	21.1
1000	2.3	4.68	6.55	9.12	11.5
1250	9.2	12.3	13.2	14.8	19.1
1600	0.9	3.27	5.05	12	28
2000	0.6	1.48	2.8	3.4	4.7
2500	0.4	1.35	2	2.52	4.4
3150	0.6	1.37	1.8	2.2	3.1
4000	0.6	1.75	2.6	3.32	12.1
5000	0.5	3.65	6.45	9.02	24.9

Table 4: Supplier 2 TDR horizontal, data for Figure 6b.

freq-band	0%	25%	50%	75%	100%
100	8.9	11.6	12.3	13.5	15.2
125	9.4	11.2	12.2	13.4	15
160	7.7	10.6	11.7	12.3	14.2
200	4.3	8	9	9.75	12
250	2.8	4.2	4.7	5.5	7.4
315	1.6	2.6	2.8	3.2	4
400	0.9	1.35	1.6	2	2.5
500	0.6	0.9	1.1	1.4	2.5
630	1.4	2.2	2.6	3.1	4.4
800	0.9	1.3	1.5	1.6	3
1000	0.4	0.5	0.6	0.7	0.9
1250	0.2	0.3	0.3	0.3	0.5
1600	0.3	0.8	0.9	1.3	3.5
2000	0.8	1	1.1	1.3	1.9
2500	0.5	1.15	1.4	1.6	2.9
3150	0.7	1.15	1.7	2.35	3.8
4000	0.7	3.25	3.9	4.55	9.7
5000	0.2	1	1.4	2	12.1